Biomedical Research (Tokyo) **38** (3) 197–205, 2017

Fine structure of human thoracic duct as revealed by light and scanning electron microscopy

Tomohiro CHIBA[1], Hirokazu NARITA[1], and Hiroshi SHIMODA[1, 2]

[1] Department of Anatomical Science and [2] Department of Neuroanatomy, Cell Biology and Histology, Hirosaki University Graduate School of Medicine, 5 Zaifu-cho, Hirosaki 036-8562, Japan

(Received 6 April 2017; and accepted 17 April 2017)

ABSTRACT

Little information has been available regarding microanatomy of human thoracic duct in spite of the importance for an understanding of pathophysiology in clinical medicine. The present study demonstrated a fine structure of human thoracic duct system by light and scanning electron microscopy. A number of longitudinal or spiral ridges and grooves were formed on luminal surfaces of the lymphangia and lymph sac, it likely facilitating fluent lymph flow. The endothelial cells displayed various cell shapes in compliance with their distributed regions. The lymph sac joining large vein composed a peculiar multiple valve structure presumably ensuring lymph storage and prevention of lymph backflow. The longitudinal muscle sheet in the tunica intima and circular muscle bundles in the tunica media constructed an integrated power unit probably eliciting spontaneous lymph propulsion. Furthermore, the thoracic duct was richly supplied with blood vessels not only in the tunica externa, but also just beneath the endothelium. The present findings provide a morphological basis for investigation of human thoracic duct in basic and clinical medicine.

The lymphatic system plays pivotal roles in physiological control of fluid homeostasis, immune surveillance and fat absorption, as well as in some pathological conditions involving lymphedema, inflammation and tumor metastasis. The lymphatic vasculature is composed of thin-walled initial segment preparing lymph in peripheral tissues (initial lymphatic, lymphatic capillary) and of the other larger one with muscle media transporting lymph centripetally to venous circulation (collecting lymphatic) (21, 23–25).

The fine structure of lymphatic capillaries has been documented in detail in various mammalian organs (15–17, 19–21). In contrast, the microanatomy of such collecting lymphatics as thoracic duct (6–9, 18), especially in humans, has been scarcely known, despite of their significance in the context of pathophysiology under clinical medicine, though their architecture has been well explored from gross anatomical point of view (4, 5). Hence, the present study demonstrates the precise microanatomical structure of human thoracic duct, a representative of collecting lymphatics, by light and scanning electron microscopy.

Address correspondence to: H. Shimoda, M.D., Ph.D., Department of Anatomical Science, Hirosaki University Graduate School of Medicine, 5 Zaifu-cho, Hirosaki 036-8562, Japan
Tel: +81-172-39-5004, Fax: +81-172-39-5006
E-mail: hshimoda@hirosaki-u.ac.jp

MATERIALS AND METHODS

The thoracic ducts were carefully dissected in five adult Japanese cadavers without macroscopicaly pathological and iatrogenic abnormalities in thoracic and epigastric regions (3 males and 2 females with ages ranging from 76 to 86 years at death). The cadavers were donated for anatomical education and researches in Hirosaki University Graduate School of Medicine, and fixed in 8% formalin and preserved in 30% alcohol. This study was conducted under the Guidelines of studies using human biomaterials and with the ethical approval of Hirosaki University (No. 2013-263). Following the dissection,

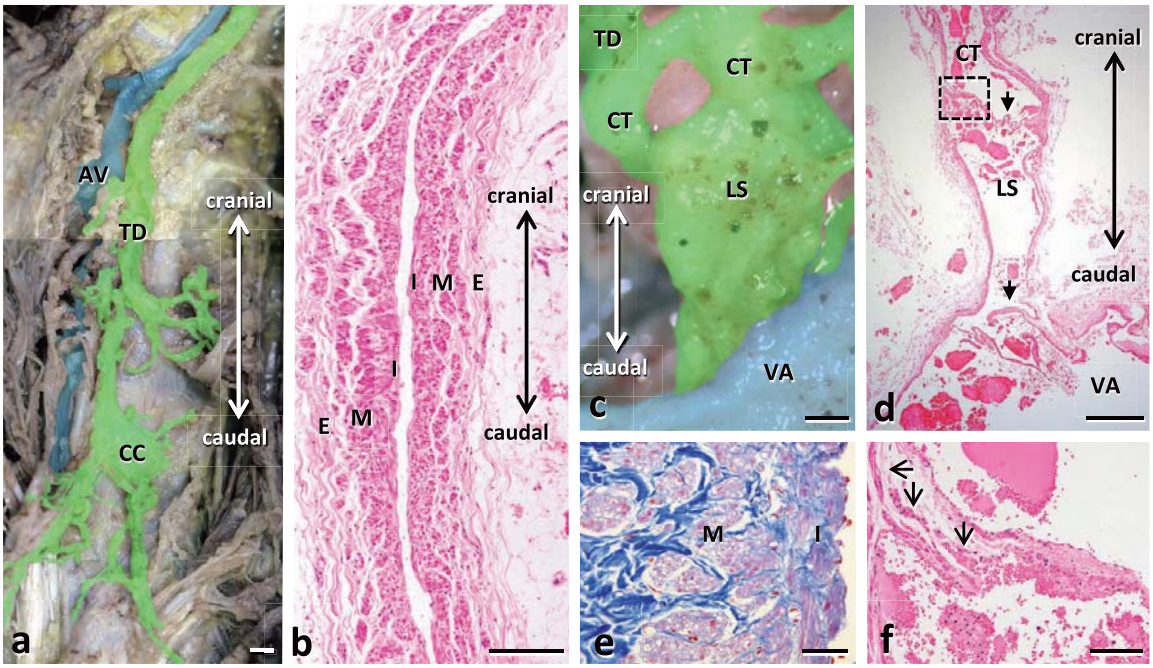

Fig. 1 Macroscopic (a, c) and microscopic (b, d–f) views of a human thoracic duct. **a**: A thoracic duct (TD) starting from Cisterna chyli (CC) extends along azygous vein (AV) in a standard course. The lymphatic and vein are colored green and blue, respectively. bar, 1 cm. **b**: A longitudinal tissue section of a thoracic duct with hematoxylin-eosin (H.E.) staining. The thoracic duct wall comprises three layers: tunica intima (I), tunica media (M) and tunica externa (E). bar, 200 µm. **c**: Jugular portion of a thoracic duct (TD) terminates to a lymph sac (LS) via connecting tubes (CT) and the sac joins to venous angle (VA) directly. The lymphatic and vein are colored green and blue, respectively. bar, 1 mm. **d**: A longitudinal tissue section of a jugular lymph sac (LS) joining to venous angle (VA) with H.E. staining. Large bicuspid valves (arrows) are seen both at entrance and exit of the sac. CT, connecting tube. bar, 1 mm. **e**: Closer view of a longitudinal tissue section of a thoracic duct wall with azan staining. The tunica intima (I) and tunica media (M) contain smooth muscles and collagenous tissue, and blood vessels are seen throughout the entire wall. bar, 50 µm. **f**: Closer view of the boxed area in **d**. Entrance valve leaflet of the lymph sac contains smooth muscles (arrows) at the base. bar, 100 µm. The double-headed arrow in **a**–**d** indicates the craniocaudal direction.

the thoracic ducts running in most standard course (Fig. 1a) were removed at all length from Cisterna chyli to venous angle and immersed in 10% neutral formalin for light microscopy or in a Karnovsky's fixative (2.5% glutaraldehyde, 2.0% paraformaldehyde, 0.1 M phosphate buffer) for scanning electron microscopy.

Light microscopy. Several tissue pieces of different sites of thoracic ducts were embedded in paraffin and cut into 5 µm thick sections. The sections were processed for hematoxylin-eosin (H.E.) and azan stainings.

Scanning electron microscopy (SEM). Some specimens fixed with Karnovsky's fixative were cut along their longitudinal direction with razor blade for observation of the luminal faces, and the others were processed for the following maceration method originated by Takahashi-Iwanaga and Fujita (22) for analysis of the mural tissue components. Briefly, they were immersed in 6N NaOH at 60°C for 15 min, stained by tannin-osmium method (10), dehydrated in a graded ethanol series, freeze-dried by t-butylalcohol, and observed under a scanning electron microscope (JSM-6510LV; JEOL, Japan).

RESULTS

The human thoracic ducts comprised basically three layers in the dissected vascular wall, and the entire wall thickness of the posteromediastinal thoracic duct was estimated 200–300 µm (Fig. 1a, b). While thin endothelium was underlain by a thin connective tissue and flat smooth muscles oriented longitudinally in the inner layer (tunica intima; I in Figs. 1b, e, 2a), a large amount of collagenous tissue and circular smooth muscle bundles constructed the middle mural layer (tunica media; M in Figs. 1b, e, 2a). The blood vessels were distributed throughout the

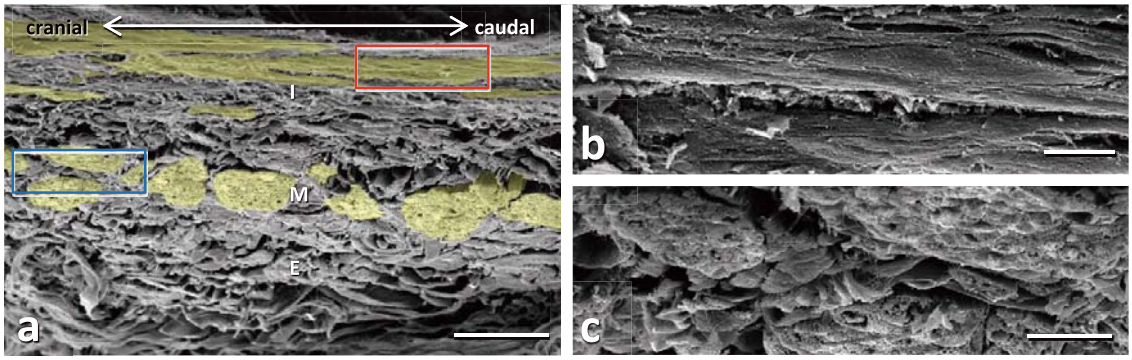

Fig. 2 SEM views of longitudinal section of a human thoracic duct. **a**: The tunica intima (I) and media (M) include longitudinal and circular muscle bundles (yellow), respectively. The double-headed arrow indicates the craniocaudal direction. bar, 50 µm. E, tunica externa. **b**, **c**: Closer views of the red and blue boxed area in a, respectively. bars, 5 µm (b), 10 µm (c).

all layers (Fig. 1e), whereas the adventitial connective tissue layer developed a vasa vasorum consisting of small arteries, small veins and capillary plexus (tunica externa; Fig. 8a–c). The jugular (terminal) portions of the thoracic ducts were joined to the saccular structures (lymph sacs; 5–7 mm in diameter; LS in Fig. 1c, d) by some connecting tubes (2–3 mm in caliber; CT in Fig. 1c, d). The lymph sacs became thinner in wall thickness (approximately 100 µm) (LS in Fig. 1d) and were equipped with large funnel-like valves at both entrance (between connecting tubes and lymph sacs) and exit (between lymph sacs and venous angles) sites (Figs. 1d, f, 5).

Luminal structure of the thoracic duct

The luminal face of the mediastinal (distal) lymphangia of human thoracic ducts showed several spiral ridges of the endothelium (Fig. 3a) and tightly laid the attenuated endothelial cells with various cellular shapes (Fig. 3b). The endothelial cells connected their diverse cell contours to each other like undulated jigsaw puzzle (Fig. 3b) and projected a number of microvilli-like processes into the lumen (Fig. 3c).

The valve portions of distal thoracic ducts often exhibited typical funnel-like valves in their lumina (V in Fig. 4a). The luminal surfaces of the valves appeared overall smooth (Fig. 4a), though some shallow grooves ran longitudinally in parts. The basal parts of the valves displayed longitudinally-elongated endothelial cells overlapping with each other by their sides (Fig. 4c), whereas rhomboid endothelial cells with circular extension contacted along their borders and entirely veiled the tip portions in proximity to exit of the valves (Fig. 4b). Although the basal parts of the valves were comparatively smooth on their luminal surfaces (Fig. 4c), plenty of microprojections were distributed on the endothelium in the valvular tip portions (Fig. 4b).

The lymphatic valves between the jugular connecting tubes and lymph sacs disclosed a complicated construction as compared to those in mediastinal thoracic ducts under SEM observation (Fig. 5a–d). The large bicuspid endothelial leaflets (primary leaflets; PL in Fig. 5a, b) formed funnel-type valves, and several distinct intraluminal folds, being relative to the valves, extended longitudinally through the valve ports from the connecting ducts to the lymph sacs (arrows in Fig. 5a). Besides those structures, some small endothelial leaflets (secondary leaflets; SL in Fig. 5a) were prepared around roots of the primary leaflets at exits of the valves to yield a small endothelial pocket (stars in Fig. 5a) being capable of storing lymph and free cells (Fig. 5b), as well as large valvular pockets (asterisks in Fig. 5a). The lymph sacs were covered with trapezoid or slender endothelial cells on their lumina as seen on the valves (Fig. 5b), whereas those of the joining region to venous angle exhibited irregularly-shaped endothelial cells like endothelium of veins (Fig. 5c–d). While the lymphatic valves were predominantly composed of endothelium and its underlying connective tissue, the inlet valves of the jugular lymph sacs disposed smooth muscles at their basal parts (Fig. 1f).

Mural structure of the thoracic ducts

The present study specifically focused on construction and the morphological characteristics of the muscular and vascular tissues in each layer of human thoracic duct. SEM examination of the human thoracic ducts after NaOH maceration allowed a precise analysis of three-dimensional structure of the cell and tissue components in the thoracic ductal wall (Figs. 6–8).

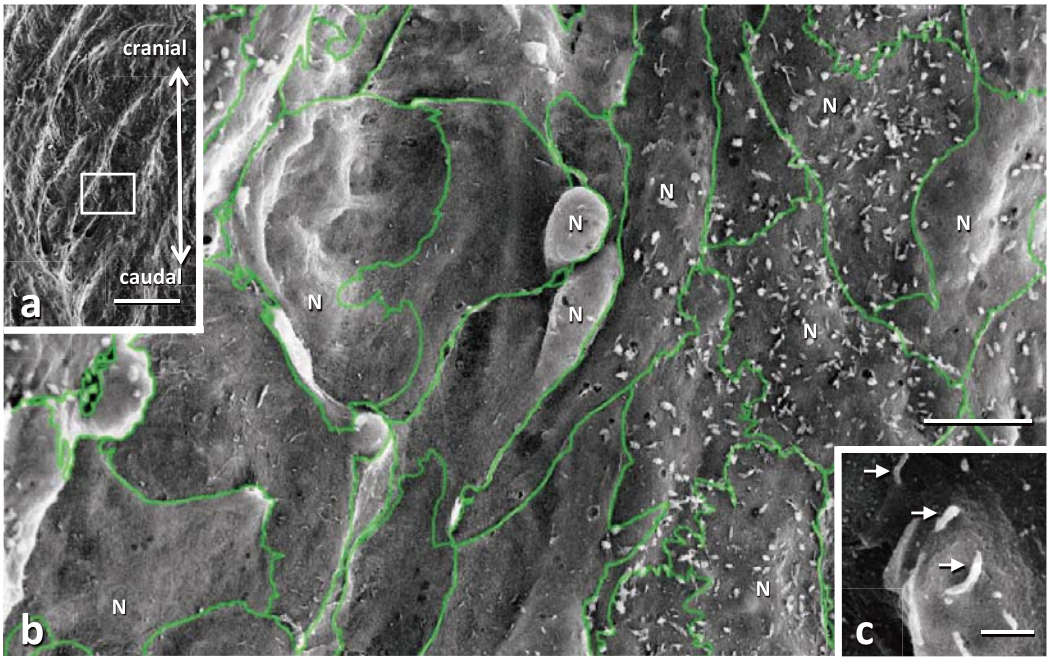

Fig. 3 SEM views of the luminal surface of a human thoracic duct. **a**: Several ridges run spirally or longitudinally on the luminal surface. The double-headed arrow indicates the craniocaudal direction. bar, 100 μm. **b**: A closer view of the boxed area in **a**. The endothelium is covered by flattened and irregularly-shaped cells contacting with each other. Many intraluminal small projections are seen on the luminal surfaces. The endothelial cell contours are colored green. N, nucleus. bar, 10 μm. **c**: Closer view of the intraluminal projections. The endothelial cells protrude microvilli-like processes (arrows). bar, 1 μm.

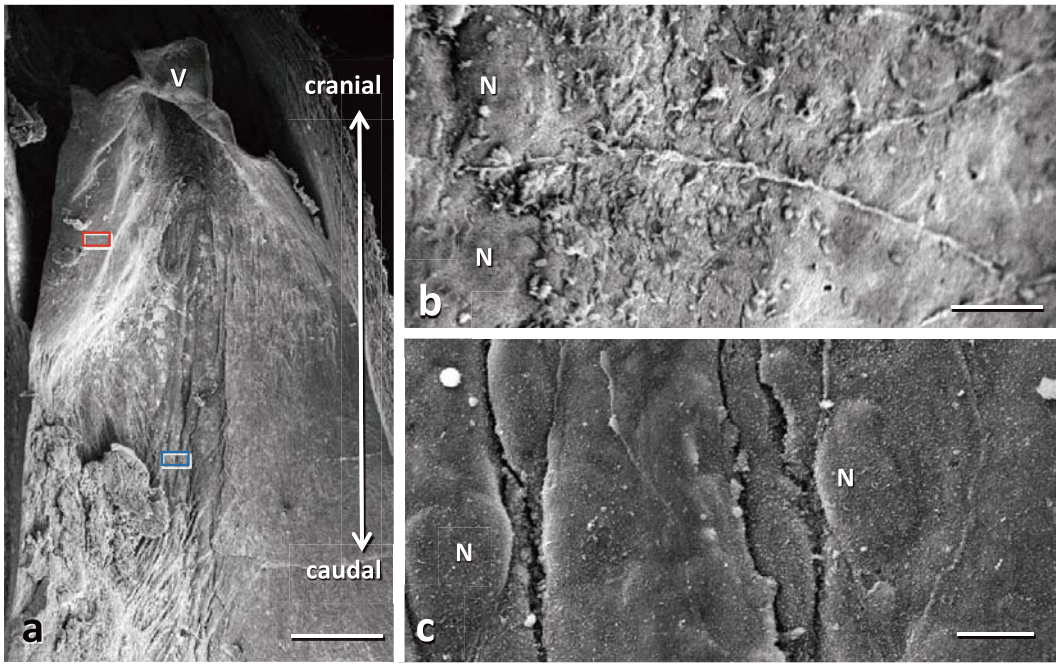

Fig. 4 SEM views of the luminal aspect at the valve portion of a human thoracic duct. **a**: A funnel-like valve (V) consisting of endothelium and its underlying connective tissue are seen within the lumen. The double-headed arrow indicates the craniocaudal direction. bar, 500 μm. **b**: Coser view of the red boxed area in **a**. Rhomboidal endothelial cells extending their long axes to the circular direction of the thoracic duct are stitched along their borders. Many intraluminal processes are seen on the endothelium. bar, 5 μm. **c**: Closer view of the blue boxed area in **a**. The endothelial cells elongate longitudinally in craniocaudal direction and overlap by their sides. N in **b**, **c**, outlines of endothelial cell nuclei. bar, 5 μm.

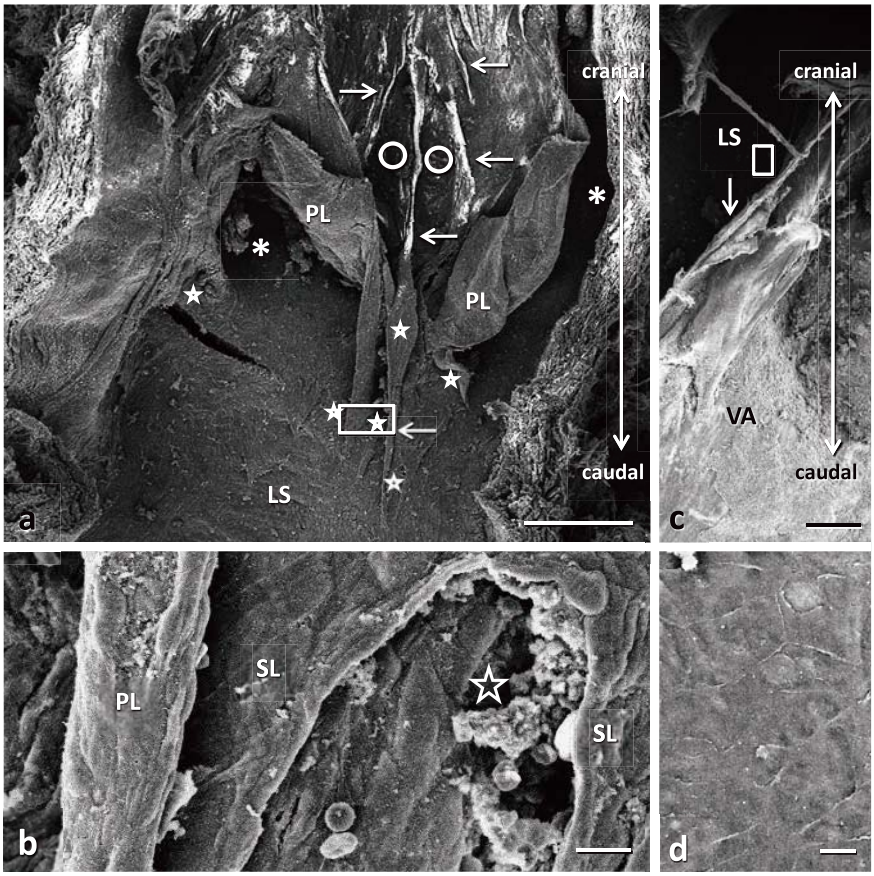

Fig. 5 SEM views of luminal aspect at entrance (a, b) and exit (c, d) portions of the lymph sac (LS) into which a human thoracic duct joins via connecting tubes shown in Fig. 1c–d. **a**: Several longitudinal folds (arrows) and grooves (circle) run through lymph pathway between large primary leaflets (PL) comprising bicuspid valve between the connecting tube and lymph sac. Large (asterisks) and multiple small (stars) pocket formations are seen concomitantly with those. bar, 500 μm. **b**: Closer view of the boxed area in **a**. The small pocket (star) surrounded by small secondary leaflets (SL) contains many cellular elements. The elongated endothelial cells contact with each other to envelop their luminal surfaces. bar, 10 μm. **c**: The lymph sac (LS) joins to venous angle (VA) through large valve (arrow). bar, 500 μm. **d**: Closer view of the boxed area in **c**. The joining region shows irregularly-shaped endothelial cells connecting continuously to each other. bar, 10 μm. The double-headed arrow in **a**, **c** indicates the craniocaudal direction.

Tunica intima. The tunica intima distributed many smooth muscles running in a longitudinal direction with some amounts of connective tissue immediately beneath the endothelium to make undulated appearances on the luminal surfaces (Figs. 2a, 6). The smooth muscle cells were flat and irregular in shape and characterized by numerous slender and/or spinous cytoplasmic projections (arrows in Fig. 6c) and numerous caveolae (arrowheads in Fig. 6c) on their rugged surfaces. They were connected with each other by their processes to form a mesh sheet-like structure intermingled with connective tissue (Figs. 1e, 2a, b, 6b) with many pores 5–15 μm in diameter (arrowheads in Fig. 6b).

In addition, a blood capillary network was well developed in the tunica intima of human thoracic duct (Fig. 8d). The blood capillaries were substantially equipped with pericytes of various shapes on their endothelial tubes. The pericytes disclosed cytoplasmic lamellae with irregular outlines and slender long processes (primary projections) running along the long axes of the vessels, with oval or fusiform nuclei portions under SEM (Fig. 8d). The primary projections further protruded numerous secondary and tertiary spines to embrace multiple endothelial tube segments loosely (Fig. 8d).

Tunica media. The muscle coat was developed with a large amount of connective tissue also in the tunica media (Figs. 1b, e, 2c, 7a–c). Although the smooth muscle cells exhibited similar profiles to those in the tunica intima other than their being spindle in

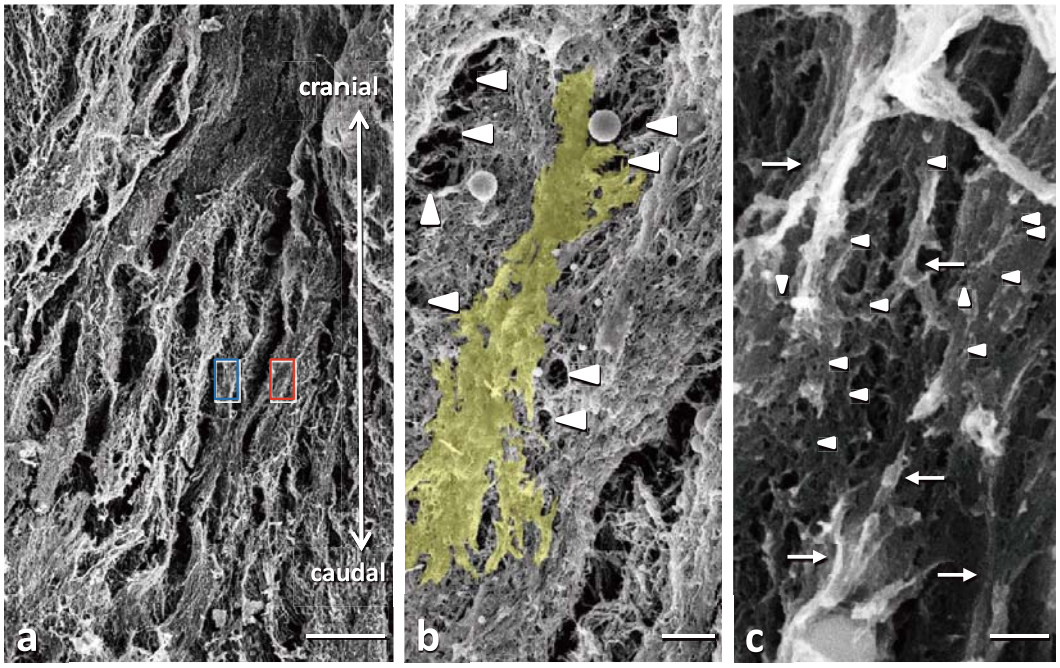

Fig. 6 SEM views of the tunica intima of a human thoracic duct from the luminal side. **a**: The membranous tissue shows many undulations beneath the endothelium. bar, 100 μm. The double-headed arrow indicates the craniocaudal direction. **b**: Closer view of the blue boxed area in **a**. Flat and irregularly-shaped muscle cells connect to each other by their cytoplasmic projections to build a thin sheet-like structure with some small pores (arrowheads). A smooth muscle cell is colored yellow. bar, 10 μm. **c**: Closer view of the red boxed area in **a**. The muscle cells show many slender processes (arrows) and elliptical or round caveolae (arrowheads) on their rough surfaces. bar, 1 μm.

shape (Fig. 7a–b), they extended in a circular fashion and concentrated into cylindrical bundles with conspicuous indented surfaces, unlike a thin sheet observed in the tunica intima (Figs. 1b, e, 2a, c, 7a–c). The circular muscle bundles somewhat roughly enveloped thoracic duct wall as compared with those of arterial or venous media (Figs. 2a, c, 7a–c). The smooth muscle bundles in the tunica media were in parts joined to the subendothelial muscle sheet with some thinner muscle bundles extending longitudinally in a craniocaudal direction and obliquely between the tunica intima and media (Fig. 7d).

Tunica externa. The tunica externa was enveloped by abundant blood vascular network, consisting of small arteries, capillaries and small veins with dense connective tissue (Figs. 1b, 8a), but no lymphatics were recognizable. The arterial and venous segments were circularly or obliquely encircled with smooth muscle cells various in shape and size (Fig. 8c), whereas the capillaries were scantily endowed with pericytes (Fig. 8b).

DISCUSSION

The present study has defined the fine structure of human thoracic ducts using light and scanning electron microscopy. Although a few reports have described the muscle coat of thoracic ducts in mammals (7, 17, 18), little, if any, information has been practically available with regard to the systematic microanatomy of human thoracic duct notwithstanding its critical importance in the fields of clinical and basic medicine. The present paper is the first to demonstrate the overall microstructure of human thoracic duct precisely in relation to gross anatomical composition, and therefore provides an anatomical basis required not only for clinical and pathophysiological investigation into human thoracic duct but also for evaluation of tissue implant in regenerative medicine.

Luminal structural profiles

The lumina of the initial portions of thoracic ducts displayed spirally-gathered aspects as compared to smooth luminal surfaces of the lymphatic capillaries (15, 16), and grooves between the ridges are likely to set fluent flow in the lymphatic transport of the

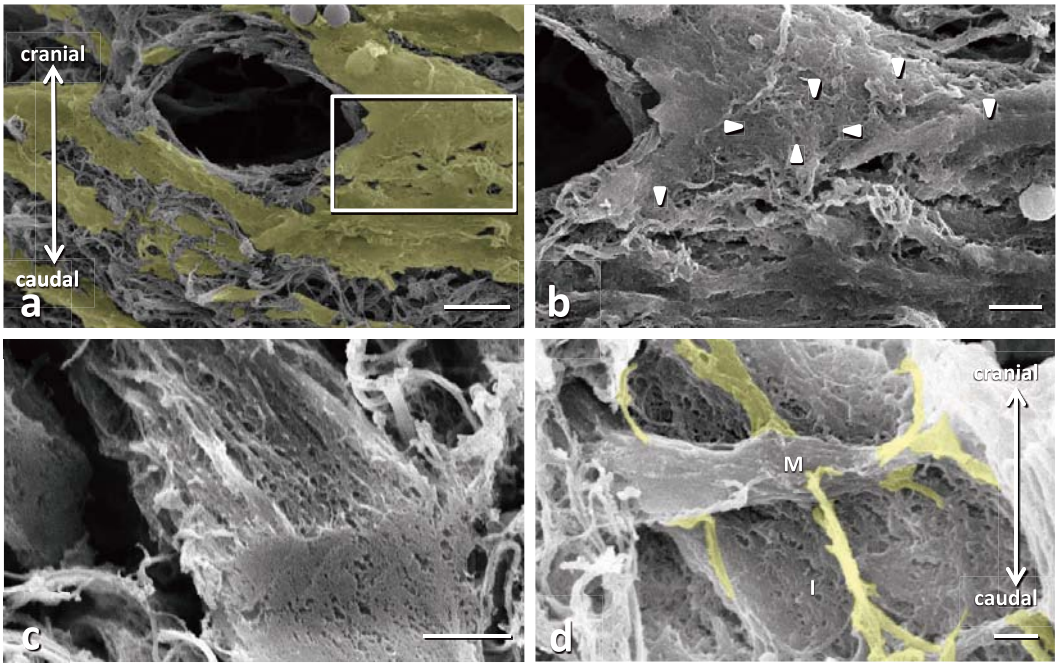

Fig. 7 SEM views of the tunica media of a human thoracic duct from the luminal (a, b) or abluminal (c, d) side. **a**: The smooth muscle cells (yellow) are spindle in shape and elongate in a circular direction. bar, 5 µm. **b**: Closer view of the boxed area in **a**. Many slender cytoplasmic projections and caveolae (arrowheads) are seen on the cellular surfaces. bar, 2 µm. **c**: The muscle bundle, a mass of the smooth muscle cells, shows cylindrical contour and highly-indented surface. bar, 10 µm. **d**: Slender longitudinal muscle bundles (yellow) connect circular muscle bundles in the tunica media (M) and a muscular sheet in the tunica intima (I). bar, 5 µm. The double-headed arrow in **a**, **d** indicates the craniocaudal direction.

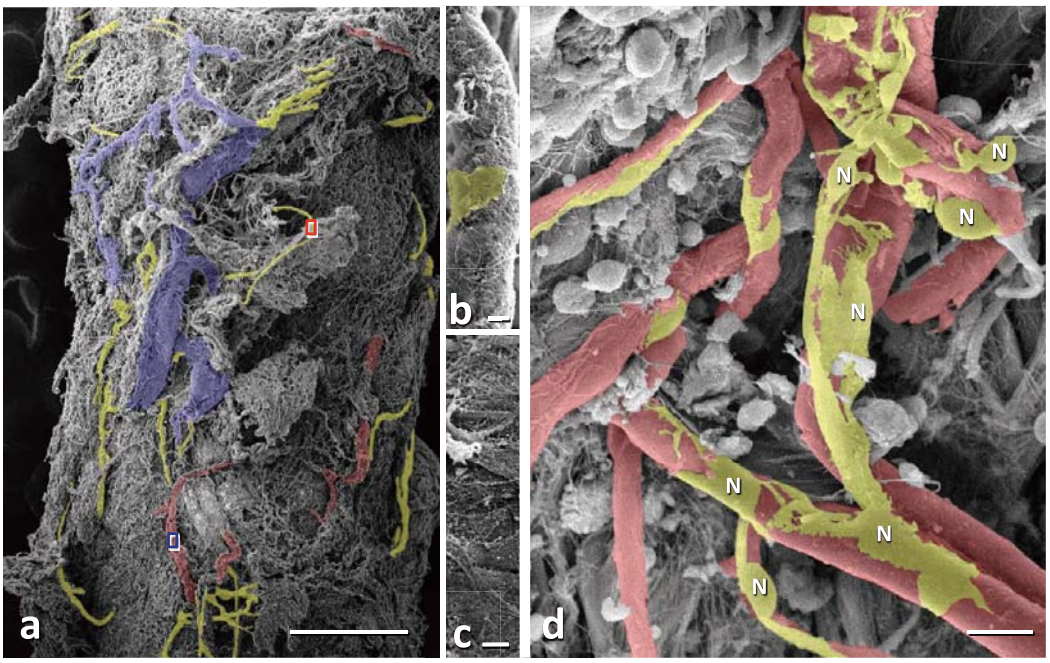

Fig. 8 SEM views of the tunicae externa (a–c) and interna (d) of a human thoracic duct from the abluminal side. **a**: A vascular network consisting of arterial (red) and venous (blue) segments and capillaries (yellow) entirely surrounds the thoracic duct wall. bar, 500 µm. **b**, **c**: Closer views of the red and blue boxed areas in **a** show investments of pericyte (yellow in **b**) in capillary (b) and of muscle media in small artery (c). bars, 1 µm. **d**: Blood capillaries (red) equipped with pericytes (yellow) extending multiple cytoplasmic branches are distributed beneath the lymphatic endothelium. N, nucleus of pericyte. bar, 10 µm.

distal thoracic duct. While contours of the endothelial cells in the thoracic duct were mostly parallel to those in lymphatic capillaries, the thoracic duct endothelium prepared a number of maculae invested with numerous microvilli. The distinctive structure might serve as a perceiver of lymph flow in the thoracic duct. Meanwhile, the area of the valves and their vicinity showed elongated or rhomboidal endothelial cells contacted tightly with each other, it being different from endothelial mode of the lymphangions, and moreover, the long axial directions of the cells on the valve tips were perpendicular to those on the valvular bases. The present findings, therefore, afford a precise configuration and array of the endothelial cells in the thoracic duct valve territory in which molecular insights into lymphatic valve development have been recently described (2, 3). This unique organization of the endothelial cells on the valves is presumed to avail for structural endurance for mechanical stress by propulsive lymph transport between distal and proximal lymphangions.

It is noteworthy that complicated multi-valvular structure consisting of large primary leaflets and small secondary ones was constituted at entrance of the lymph sacs joining to large veins. The multiple folds longitudinally running along the passage between primary valve leaflets are supposedly valuable for provision of proper lymph flow channel by arranging some trenches and for tight closure of the valve checking lymph backflow. Several small secondary leaflets and their pocket formation subordinate to the large primary ones are also likely to help in lymph retention and prevention of lymph back flow. It is presumably accommodated to the functional roles that the endothelial cells in the lymph sacs assumed similar morphological aspects to those of the lymphatic valves rather than in the lymphangions and veins.

Mural structural profiles

In human thoracic duct, the smooth muscles were disposed longitudinally in their orientation in the tunica intima and circularly in the tunica media, thus the muscular organization resembling that of venous wall. The tunica intima, however, composed a peculiar mesh sheet structure of longitudinal smooth muscles, and it perhaps contributes to formation of the longitudinal luminal folds in cooperation with circular muscle bundles in the tunica media as well as preservation of the luminal configuration. In addition, abundant tiny pores of the muscular sheet may afford pathways for vessels, free cells and tissue fluid.

In contrast, the circular muscle bundles in the tunica media were firmly united to the surrounding connective tissue by their prominent surface indentation, thereby implying that the substantial muscle coat is pivotal to produce intraluminal pressure waves propelling lymph fluid and phasic motion of the lymphangions for lymph propulsion (11). Furthermore, of special note is the occurrence of longitudinal muscular bundles connecting the intimal muscular sheet and medial muscle bundles, and they likely permit coordination of the muscular components between the tunicae intima and externa. Hence, the integrated muscular device maybe provides spontaneous contraction of the thoracic duct (1, 12) to regulate proper lymph flow with sustaining the ductal figure. In addition, an exceptional equipment of smooth muscles at base of the inlet valves of the jugular lymph sac conceivably serve as a valvular motor unit for constriction of the valve ring and strict prevention of lymph and blood backflow.

The human thoracic duct further demonstrated a dense network of capillaries complicatedly folded by the pericytes with various cytoplasmic branches beneath the endothelium, along with a well-developed vasa vasorum in the tunica externa (13). Since the partial oxygen pressure in lymph in the thoracic duct has been previously reported to be lower than that in venous blood (14), a rich blood-oxygen-supply through the vascular network to the muscular components is probably crucial for the transporting and recruiting activity of lymph.

REFERENCES

1. Azuma T, Ohhashi T and Sakaguchi M (1977) Electrical activity of lymphatic smooth muscles. *Proc Soc Exp Biol Med* **155**, 270–273.
2. Bazigou E, Wilson JT and Moore Jr JE (2014) Primary and secondary lymphatic valve development: Molecular, functional and mechanical insights. *Microvac Res* **96**, 38–45.
3. Cha B, Geng X, Mahamud MR, Fu J, Mukhejee A, *et al.* (2016) Mechanotransduction activates canonical Wnt/β-cateinn signaling to promote lymphatic vascular patterning and development of lymphatic lymphvenous valves. *Genes Dev* **30**, 1454–1469.
4. Kihara T (1953) Das Lymphgefäßsystem der Japaner von Buntaro Adachi, Kenkyusha, Tokyo.
5. Kihara T (1963) Das tiefe Lymphgefäßsystem der Japaner. Deutch-Japanisches Kulturinstitut, Kyoto.
6. Kim J-H, Han E-H, Jin Z-W, Lee H-K, Fujimiya M, *et al.* (2012) Fetal topographical anatomy of the upper abdominal lymphatics: its specific features in comparison with other abdominopelvic regions. *Anat Rec* **295**, 91–104.
7. Lee SH, Wen HJ and Shen CL (1993) Ultrastructure of the monkey thoracic duct and the cisterna chyli. *J Anat* **182**, 205–212.
8. Mihara M, Hara H, Hayashi Y, Narushima M, Ymamoto T,

Todokoro T, *et al.* (2012) Pathological steps of cencer-related lymphedema: Histological changes in the collecting lymphatic vessels after lymphadectomy. *Plos One* **7**, e41126.
9. Mihara M, Hara H, Kikuchi K, Narushima M, Yamamoto T, *et al.* (2012) Indocyanine green (ICG) lymphography is superior to lymphocintigraphy for diagnostic imaging of early lymphedema of the upper limbs. *Plos One* **7**, e38172.
10. Murakami T (1974) A revised tannin-osmium method for non-coated scanning electron microscope specimens. *Arch Histol Jpn* **36**, 189–193.
11. Negrini D and Moriondo A (2011) Lymphatic anatomy and biomechanics. *J Physiol* **589**, 2927–2934.
12. Ohhashi T, Azuma T and Sakaguchi M (1980) Active and passive mechanical characteristics of bovine mesenteric lymphatics. *Am J Physiol* **239**, H88-H95.
13. Ohhashi T, Fukushima S and Sakaguchi M (1977) Vasa vasorum within media of bovine mesenteric lymphatics. *Proc Soc Exp Biol Med* **154**, 582–586.
14. Ohhashi T, Mizuno R, Ikomi F and Kawai Y (2005) Current topics of physiology and pharmacology in the lymphatic system. *Pharmacol Ther* **105**, 165–188.
15. Ohtani O (1987) Three-dimensional organization of lymphatics and its relationship to blood vessels in rat small intestine. *Cell Tissue Res* **248**, 365–374.
16. Ohtani O and Murkami T (1990) Organization of the lymphatic vessels and their relationships to blood vessels in rabbit Peyer's patches. *Arch Histol Cytol* **53** (Suppl), 155–164.
17. Ohtani O and Ohtani Y (2008) Organization and developmental aspects of lymphatic vessels. *Arch Histol Cytol* **71**, 1–22.
18. Shimada K and Sato I (1997) Morphological analysis of the thoracic duct at the jugulo-subclavian junction in Japanese cadavers. *Clin Anat* **10**, 163–172.
19. Shimoda H (1998) Structural organization of lymphatics in the monkey esophagus as revealed by enzyme-histochemistry. *Arch Histol Cytol* **61**, 439–450.
20. Shimoda H (2009) Immunohistochemical demonstration of angiopoietin-2 in lymphatic vascular development. *Histochem Cell Biol* **131**, 231–238.
21. Shimoda H and Kato S (2006) A model for lymphatic regeneration in tissue repair of the intestinal muscle coat. *Int Rev Cytol* **250**, 73–108.
22. Takahashi-Iwanaga H and Fujita T (1986) Application of an NaOH maceration method to scanning electron microscopic observation of Ito cells in the rat liver. *Arch Histol Jpn* **49**, 349–357.
23. Tammela T and Alitalo K (2010) Lymphangiogenesis: Molecular mechanisms and future promise. *Cell* **140**, 460–476.
24. Ulvmar MH and Mäkinen T (2016) Heterogeneity in the lymphatic vascular system and its origin. *Cardiovasc Res* **111**, 310–321.
25. Yan Y and Oliver G (2014) Development of the mammalian lymphatic vasculature. *J Clin Invest* **124**, 888–897.